ACS OMEGA

http://pubs.acs.org/journal/acsodf

Article

Clusteromics V: Organic Enhanced Atmospheric Cluster Formation

Daniel Ayoubi, Yosef Knattrup, and Jonas Elm*

Cite This: *ACS Omega* 2023, 8, 9621−9629

Read Online

ACCESS | Metrics & More | Article Recommendations | Supporting Information

ABSTRACT: Formic acid (FA) is a prominent candidate for organic enhanced nucleation due to its high abundance and stabilizing effect on smaller clusters. Its role in new particle formation is studied through the use of state-of-the-art quantum chemical methods on the cluster systems $(acid)_{1-2}(FA)_1(base)_{1-2}$ with the acids being sulfuric acid (SA)/methanesulfonic acid (MSA) and the bases consisting of ammonia (A), methylamine (MA), dimethylamine (DMA), trimethylamine (TMA), and ethylenediamine (EDA). A funneling approach is used to determine the cluster structures with initial configurations generated through the ABCluster program, followed by semiempirical PM7 and ωB97X-D/6-31++G(d,p) calculations. The final binding free energy is calculated at the DLPNO-CCSD(T_0)/aug-cc-pVTZ//ωB97X-D/6-31++G(d,p) level of theory using the quasi-harmonic approximation. Cluster dynamics simulations show that FA has a minuscule or negligible effect on the MSA−FA−base systems as well as most of the SA−FA−base systems. The SA−FA−DMA cluster system shows the highest influence from FA with an enhancement of 21%, compared to its non-FA counterpart.

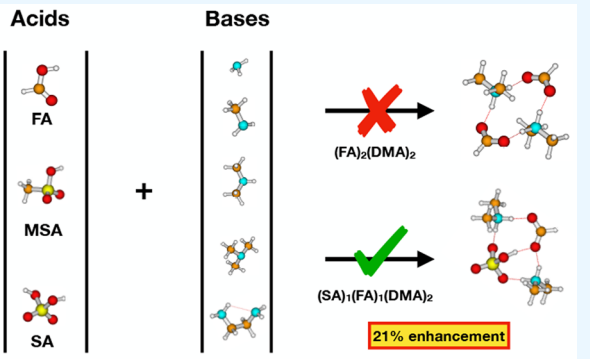

1. INTRODUCTION

Aerosol particles play a significant role in global climate due to their direct impact on solar radiation[1] and their ability to act as nuclei for cloud droplet formation.[2] The clustering of low volatile acid molecules with atmospheric base molecules is the primary factor in the formation of new atmospheric particles (NPF), which provide the necessary surface for initiating cloud droplet formation. Studies have shown that NPF accounts for approximately half of the global concentration of cloud condensation nuclei (CCN).[3] However, the compounds involved in the formation and growth of atmospheric aerosols are not well understood, leading to significant uncertainty in global climate estimates.[4] Sulfuric acid (SA) has been extensively studied through quantum chemical calculations and its ability to cluster with atmospheric base molecules is well established as a key factor in NPF.[5−21] Methanesulfonic acid (MSA) has received less attention than SA, but it has been the subject of significant research recently.[22−32] Despite the potential significance of atmospheric multicomponent clusters comprising multiple acids and bases, they have received relatively little attention. Quantum chemical studies have indicated that the inclusion of MSA in clusters with SA is capable of enhancing the cluster formation potential.[33−35] Organic acids have been proposed to enhance SA-driven NPF[36] and have resulted in great interest in understanding organic-enhanced NPF. However, with a large number of organic compounds in the atmosphere, it is difficult to assess which are of importance in NPF. Currently, no organic compound has been proven to be a strong nucleator. Nonetheless, formic acid (FA) is a relevant organic acid to investigate due to its hydrogen bonding capability[37] and its high abundance in the atmosphere ranging from 2.50×10^9 to 3.75×10^{11} molecules cm^{-3}.[38] Similarly to nitric acid, previously studied,[35] this is orders of magnitude higher than the 10^5 to 10^7 molecules cm^3 that has been measured for SA and MSA.[39−41] Nadykto and Yu[37] were the first to investigate the interaction between atmospheric nucleation precursors (sulfuric acid, ammonia, water) and common carboxylic acids (formic and acetic acid) using quantum chemical methods. From their calculations, they suggested that FA had a stabilizing effect similar to that of ammonia (A), indicating that these organic acids may effectively stabilize small SA−water clusters. Harold et al.[42] examined the possibility that acids and bases may exhibit different behavior at the nanoscale than in a bulk solution. Calculations of binding free energies and steady-state cluster concentrations for various combinations of FA, SA, A, and water (W) were performed. In line with Nadykto and Yu, they found that formic acid was able to stabilize clusters containing SA and W to the same extent as A. Additionally, they concluded that hydrogen bonding topology played an important role in determining the stability of these

Received: January 13, 2023
Accepted: February 17, 2023
Published: February 28, 2023

https://doi.org/10.1021/acsomega.3c00251
ACS Omega 2023, 8, 9621−9629

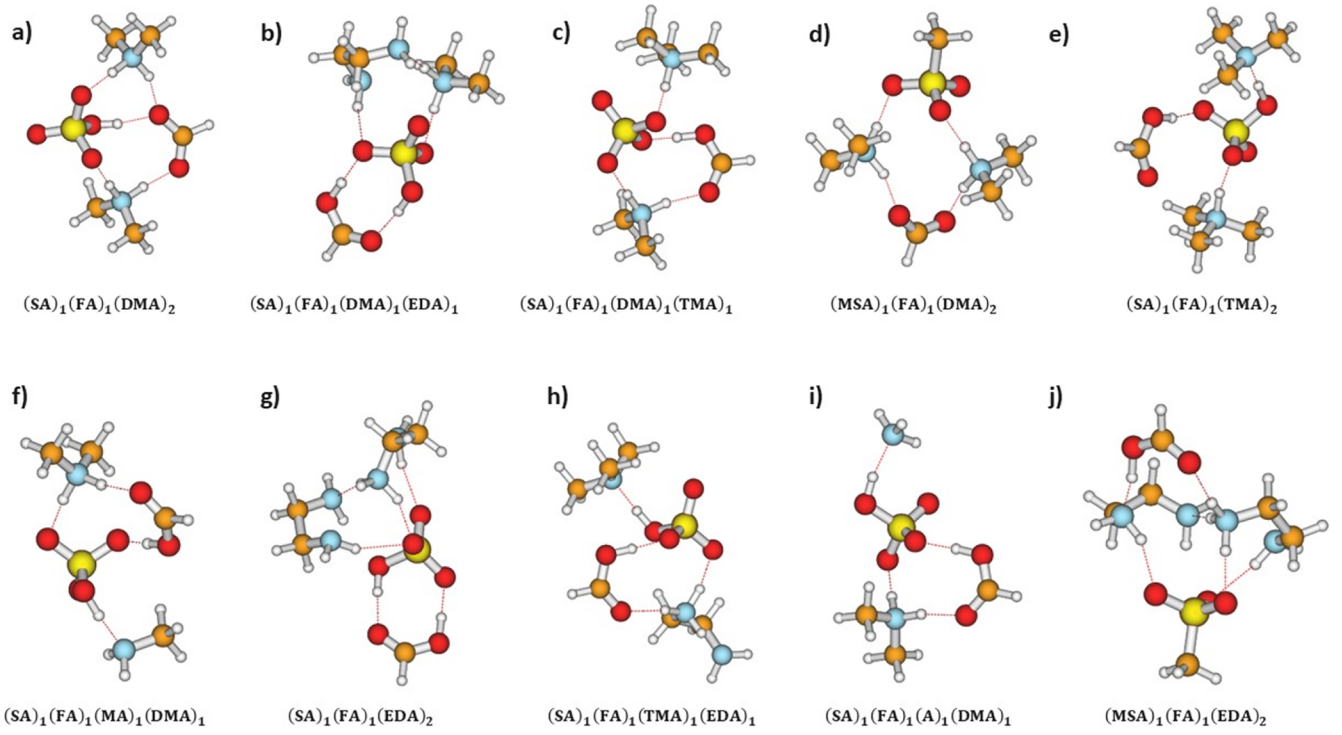

Figure 1. (a–j) Calculated lowest free energy (298.15 K, 1 atm) cluster structures at the DLPNO–CCSD(T_0)/aug-cc-pVTZ//ωB97X-D/6-31++G(d,p) level of theory using the quasi-harmonic approximation.

clusters. They also found that when FA and A concentrations exceeded 10^7 cm^{-3}, clusters containing SA, A, and FA were predicted to form in the upper troposphere at low temperatures and may be involved in the process of NPF. Zhang et al.[43] similarly studied the formation of multicomponent clusters between atmospheric precursors SA, dimethylamine (DMA), water, and FA. Kinetic simulations with varying FA concentrations (0.2–20 ppb) showed the effect on the steady-state concentration of the SA–dimer with higher FA concentration leading to a reduced SA–dimer concentration. The interaction of FA and the SA–DMA was stronger than that of water and the SA–DMA dimer. While the interaction of FA with the SA–DMA cluster was shown to be rather weak, the impact of FA was non-negligible on the aerosol nucleation cluster population due to its high concentration. Zhang et al.[44] showed that FA have the highest stabilizing effect on MSA–MA clusters out of 12 common atmospheric organic acids. They attributed the high atmospheric abundance, acidity, H-bond capacity, absence of no intramolecular interaction, and little/no structural deformation during clustering to properties of FA that made it a suitable candidate for NPF. Further simulations using the atmospheric cluster dynamics code (ACDC) found FA to exert a catalytic effect in the formation of small binary MSA–MA clusters, i.e., a single formic acid participates in the cluster formation but not in cluster growth, as the formic acid tends to evaporate.

The clusteromics series[34,35,45,46] has focused on the investigation of atmospheric clusters and their properties. The current paper, the fifth in the series, continues this line of research by examining multicomponent clusters comprising a combination of FA, SA, and MSA along with different nitrogen-containing bases. The bases considered are consisting of ammonia (A), methylamine (MA), dimethylamine (DMA), trimethylamine (TMA), and ethylenediamine (EDA). FA was chosen based on its high abundance in the atmosphere and previous studies indicating its role in NPF.[37,42–44] As well as FA being the simplest carboxylic acid allowing to probe the direct interactions between cluster and organic acids. The placement of FA could highlight ideal contact points for larger polyfunctional organic acids in the cluster. Thermodynamics and kinetics of the initial stages of potential cluster formation for the cluster types $(acid)_{1-2}(base)_{1-2}$ and $(acid)_3(base)_2$ in which at least one of the acids is FA and the remaining is SA or MSA will be examined in this paper.

2. COMPUTATIONAL DETAILS

Geometry optimizations and vibrational frequency calculations for density functional theory and semiempirical PM7[47] were performed using Gaussian 16.[48] The default convergence criteria of Gaussian 09[49] were employed in order to facilitate comparison with data in the Atmospheric Cluster DataBase (ACDB).[50] The ORCA 4.2.1 program[51,52] was utilized to calculated the domain-based local pair natural orbital DLPNO-CCSD(T_0)[53,54] single-point energies using a TightSCF convergence criteria[55] with the aug-cc-pVTZ basis set. The ωB97X-D functional[56] and the 6-31++G(d,p) basis set[57,58] were used for obtaining the cluster structures and vibrational frequencies, based on multiple benchmarks.[59–61] Vibrational frequencies below 100 cm^{-1} were treated with Grimme's quasi-harmonic approximation[62] using the GoodVibes[63] code. The funneling workflow used in this work is similar to the previous clusteromics papers and for a more in-depth description, the reader is referred to these[34,35,45,46] and our recent review.[64] We applied the following workflow to sample the cluster configurations:

https://doi.org/10.1021/acsomega.3c00251
ACS Omega 2023, 8, 9621–9629

Table 1. Calculated Binding Free Energies at the DLPNO-CCSD(T_0)/aug-cc-pVTZ//ωB97X-D/6-31++G(d,p) Level of Theory with the Quasi-harmonic Approximation at 298.15 K, 1 atm (Units Are kcal/mol)

	classification	$(SA)_1(FA)_1$	$(MSA)_1(FA)_1$	$(FA)_1$	$(FA)_2$
$(A)_1$	w	−14.4	−8.1	−1.1	−1.7
$(MA)_1$	m	−15.5	−12.7	−1.3	−3.7
$(DMA)_1$	s	−19.8	−15.9	−1.9	−3.5
$(TMA)_1$	s	−17.6	−14.0	−3.1	−2.2
$(EDA)_1$	s	−18.4	−14.9	−2.8	−2.7
$(A)_2$	w, w	−13.2	−10.9	1.6	1.0
$(MA)_2$	m, m	−17.8	−15.3	1.7	−0.75
$(DMA)_2$	s, s	−25.0	−21.7	1.8	−7.0
$(TMA)_2$	s, s	−21.0	−9.6	2.6	1.9
$(EDA)_2$	s, s	−20.7	−20.0	1.4	−2.7
$(A)_1(MA)_1$	w, m	−17.9	−14.3	1.9	−0.4
$(A)_1(DMA)_1$	w, s	−20.4	−15.7	1.6	−2.0
$(A)_1(TMA)_1$	w, s	−18.0	−11.6	2.2	0.7
$(A)_1(EDA)_1$	w, s	−18.7	−16.1	1.1	−1.2
$(MA)_1(DMA)_1$	m, s	−20.8	−18.8	0.6	−2.2
$(MA)_1(TMA)_1$	m, s	−19.4	−14.8	2.1	−1.3
$(MA)_1(EDA)_1$	m, s	−19.8	−18.1	1.6	−2.0
$(DMA)_1(TMA)_1$	s, s	−23.2	−15.3	1.3	−0.5
$(DMA)_1(EDA)_1$	s, s	−23.4	−19.3	0.2	−5.3
$(TMA)_1(EDA)_1$	s, s	−20.7	−13.8	1.5	−1.2

$$\text{ABCluster} \rightarrow \text{PM7} \rightarrow \text{sort} \rightarrow \text{DFT} \rightarrow \text{restart} \rightarrow \text{sort} \rightarrow \text{inspection} \rightarrow \text{DLPNO} \quad (1)$$

We used ABCluster[65,66] to perform initial calculations with the recommended settings from Kubečka et al.,[67] which included a population size of 3000 (SN = 3000), a maximum of 200 generations (g_{max} = 200), and 4 scout bees (g_{limit} = 4). For each cluster protonation state, we saved a total of 1000 local minima. These minima structures were then geometry optimized using the PM7 method and the ArbAlign[68] program was subsequently used to sort the cluster configurations and remove duplicates based on root-mean-square deviations (RMSD) between atomic positions. An RMSD cutoff of 0.38 was used as suggested by previous studies.[69,70] Energy calculations and geometry optimization of the remaining structures were then performed and rerun until convergence at the DFT level, which was then followed by a secondary sorting with the ArbAlign program to further reduce the number of redundant structures. The binding energies of the five cluster structures with the lowest free energy at the DFT level were then evaluated at the DLPNO-CCSD(T_0)/aug-cc-pVTZ level of theory.

2.1. Atmospheric Cluster Dynamics Code. The ACDC[71,72] was utilized to simulate the cluster formation potential ($J_{potential}$) using the calculated thermochemical parameters ΔH and ΔS as inputs. The software was downloaded and modified from the ACDC repository[72−74] and was employed in line with our previous research.[34,35,45,46] In the simulations, clusters with a composition of $(acid)_3(base)_{2-3}$ were included and allowed to contribute to the cluster formation potential by leaving the simulation box. However, clusters with the composition of $(acid)_2(base)_3$ were excluded as contributors to $J_{potential}$ due to their instability in electrically neutral acid−base clusters.[19,72] Default values for coagulation losses typical of the boundary layer (cs_exp = −1.6 and cs_ref = 1×10^{-3}) were also used. The simulation was run at a temperature of 278.15 K. Additional runs at 298.15 K are shown in the Supporting Information. We emphasize that the calculated flux out of the system is purely a "potential" to form larger clusters and should not be used as a measure for the actual cluster formation rate J. Besel et al.[75] recently showed that the simulated cluster formation rate increased as the simulation system was decreased. Hence, the presented $J_{potential}$ values might be artificially larger than the actual J.

3. RESULTS AND DISCUSSION

3.1. Cluster Structures. Applying the above-mentioned funneling approach, a total of 27 995 unique $(acid)_{1-2}(base)_{1-2}$ and $(acid)_3(base)_2$ cluster structures were identified. All cluster structures and their thermochemical data have been added to the ACDC database.[50] Figure 1 displays the 10 $(acid)_{1-2}(base)_{1-2}$ cluster systems with the lowest binding free energy at the DLPNO-CCSD(T_1)/aug-cc-pVTZ//ωB97X-D/6-31++G(d,p) level of theory. As demonstrated in Figure 1, the most stable clusters exhibit a network of hydrogen bonds between acids and bases with SA forming the most stable clusters, with 8 out of the 10 clusters in Figure 1 containing SA rather than MSA. A general trend observed among the $(SA)_1(FA)_1(base)_2$ clusters is the triangular interaction between SA, FA, and the base for which the most favorable hydrogen bond to FA and SA can be made, while the other base is oriented away from the core of the cluster via a hydrogen bond to SA. The selection of the base for interaction with SA and FA is based on the base strength and steric effects. For example, in the $(SA)_1(FA)_1(DMA)_1(TMA)_1$ and $(SA)_1(FA)_1(TMA)_1(EDA)_1$ clusters, the more crowded TMA is directed away from the core of the cluster via SA being positioned in the middle. This is not possible for MSA to the same extent and attributes to the lower stability of the MSA clusters. However, common for all of the studied clusters is the trend of guiding the large methyl groups away from the cluster core, resulting in the exterior of the cluster being comprised of organic side chains, which is consistent with previous findings.[34,45,46] This could imply that additional collisions toward the cluster might be less favorable due to the limited number of available H-bonding sites. However, molecular

https://doi.org/10.1021/acsomega.3c00251
ACS Omega 2023, 8, 9621−9629

dynamics simulations are required to study this effect in details. Also in accordance with our previous studies is the observed lack of acid−acid interaction in clusters containing MSA. Specifically, we do not see any interaction between FA and MSA, while we commonly observe an interaction between SA and FA. In certain clusters, we observe that the FA molecule is only interacting with sulfuric acid via a pair of donor−acceptor hydrogen bonded interactions and is not interacting with any of the base molecule. This is seen in the $(SA)_1(FA)_1(DMA)_1(EDA)_1$ and $(SA)_1(FA)_1(EDA)_2$ clusters, where base−base interactions are also observed. These types of interactions were not observed in our previous study on the role of nitric acid (NA) in cluster formation.[35] It should noted that, unlike in the previous study of NA, FA is usually not found to be deprotonated in the clusters, except in cases where it is interacting with two strong bases, such as DMA, in which proton transfer was observed.

3.2. Thermochemistry. Table 1 shows the calculated binding free energies for the $(acid)_{1-2}$ $(base)_{1-2}$ clusters at the DLPNO-CCSD(T_0)/aug-cc-pVTZ//ωB97X-D/6-31++G-(d,p) level of theory with the quasi-harmonic approximation at 298.15 K, 1 atm. The classification column refers to the basicity of the bases in the gas phase,[76] with w indicating a weak base, m is medium, and s is strong. A similar trend in binding free energy for the $(SA)_1(FA)_1(base)_1$ $(MSA)_1(FA)_1(base)_1$ clusters are observed with the following order of stability: $(A)_1$ < $(MA)_1$ < $(TMA)_1$ < $(EDA)_1$ < $(DMA)_1$. This could indicate that steric effects already take palce in these smaller clusters, with the binding free energy of the three strong bases following the order of bulkiness. This effect is not pronounced in the smaller $(FA)_1(base)_1$ clusters where TMA and EDA form the most stable interactions, as expected based on their gas-phase basicity. However, for the $(FA)_2(base)_1$ clusters the limited number of hydrogen bond donors from FA results in clusters containing the bulky TMA and EDA to become less stable than those of $(FA)_2(MA)_1$ and $(FA)_2(DMA)_1$. The $(FA)_{1-2}(base)_2$ clusters in general show high binding free energies with many of the clusters exhibiting a positive value. This lies in contrast to our previous work on the role of NA in cluster stability, in which NA showed to stabilize all studied $(NA)_{1-2}(base)_{1-2}$ clusters except those were bases only consisted of ammonia.[35] The lower stability of the FA-containing clusters compared to those in our previous study with NA, is generally observed through all the clusters in Table 1. This is likely a result of NA being a stronger acid than FA. Bready et al.[77] recently studied multicomponent clusters containing both SA, FA and NA and found that at certain conditions NA can participate as efficiently as SA in cluster formation. The results implied that cluster formation in the atmosphere is a multicomponent process that involves numerous different acid and base molecules. Recently Zhang et al.[44] have shown FA to enhance the NPF for MSA−MA clusters through a catalytic effect on small binary MSA−MA clusters in which it initially stabilizes the cluster and then evaporates off as the cluster grows. In fact, the $(SA)_1(FA)_1(base)_1$ trimer clusters show relatively high stability for the cases of the base being either A, MA or DMA (−14.4, −15.5, −19.8 kcal mol^{-1}, respectively), related to the corresponding clusters in our previous study with NA (−5.4, −13.7, 17.3 kcal mol^{-1}, respectively). This could support the claim of Zhang et al.[44] for which FA is able to stabilize smaller clusters allowing for further growth.

For the $(SA)_1(FA)_1(A)_1(base)_1$ clusters, the stability follows the pattern $(MA)_1$ < (TMA) < $_1$ < $(EDA)_1$ < $(DMA)_1$. For the $(MSA)_1(A)_1(base)_1$ clusters, the limited hydrogen bonding capacity of MSA compared to SA is revealed as ranking of the binding free energy switches between the two lowest and two highest clusters: $(TMA)_1$< $(MA)_1$< $(DMA)_1$< $(EDA)_1$. As EDA contains an extra amino group it is able to compensate for MSA's reduced hydrogen bond capacity while TMA is only able to contribute with one hydrogen bond and an unfavorable interaction between MSA and TMA is observed. This is especially pronounced for the $(MSA)_1(FA)_1(TMA)_2$ cluster which binding free energy is only −9.6 kcal mol^{-1}. The $(acid)_2(MA)_1(base)_1$ clusters follow: $(TMA)_1$ < $(EDA)_1$ < $(DMA)_1$. An aversion for TMA is still observed for these clusters and this trend continues for the rest of the clusters. For instance, for the cluster system $(acid)_1(FA)_1(DMA)_1(base)_1$, where acid is either SA, MSA or FA, having TMA in the cluster results in a higher binding free energy compared to having either DMA or EDA. The general trend of Table 2 is that for smaller clusters the decisive factor is the strength of the acid−base interaction while the effect of steric hindrance becomes more important as the size of the system increases. This is in line with previous findings[34,35,45,46] along with the observed preference for DMA and EDA at larger cluster sizes and an aversion for TMA.

Table 2. Addition Free Energies at the DLPNO-CCSD(T_0)/aug-cc-pVTZ//ωB97X-D/6-31++G(d,p) Level of Theory with the Quasi-harmonic Approximation at 298.15 K, 1 atm (Units Are kcal/mol)[a]

initial cluster:	$(SA)_1$		$(MSA)_1$		$(FA)_1$
added acid:	(SA)[45]	(FA)	(MSA)[46]	(FA)	(FA)
$(A)_1$	−13.8	−8.8	−9.0	−4.7	−0.6
$(MA)_1$	−17.2	−8.3	−13.9	−8.8	−2.4
$(DMA)_1$	−17.9	−8.3	−14.5	−8.8	−1.6
$(TMA)_1$	−15.3	−5.0	−10.4	−5.3	0.9
$(EDA)_1$	−17.7	−8.0	−15.7	−7.8	0.1
$(A)_2$	−17.3	−3.5	−17.9	−8.3	−0.6
$(MA)_2$	−25.9	−7.1	−24.1	−7.9	−2.5
$(DMA)_2$	−29.1	−10.1	−24.6	−9.7	−8.8
$(TMA)_2$	−26.2	−5.7	−19.6	−3.6	−0.7
$(EDA)_2$	−25.5	−4.4	−21.5	−7.1	−4.1
$(A)_1(MA)_1$	−22.4	−7.9	−19.4	−7.6	−2.3
$(A)_1(DMA)_1$	−21.3	−7.9	−23.6	−10.4	−3.6
$(A)_1(TMA)_1$	−18.7	−4.4	−15.5	−4.0	−1.5
$(A)_1(EDA)_1$	−20.9	−5.9	−18.2	−7.0	−2.3
$(MA)_1(DMA)_1$	−26.4	−6.6	−23.1	−8.1	−2.8
$(MA)_1(TMA)_1$	−24.7	−6.0	−20.7	−7.4	−3.4
$(MA)_1(EDA)_1$	−25.7	−6.4	−22.5	−8.4	−3.6
$(DMA)_1(TMA)_1$	−27.5	−8.4	−20.7	−5.3	−1.8
$(DMA)_1(EDA)_1$	−26.0	−6.0	−24.7	−8.6	−5.5
$(TMA)_1(EDA)_1$	−27.6	−5.6	−21.3	−5.5	−2.7

[a]Calculated as the initial cluster binding free energy subtracted from the binding free energy of the cluster with the added acid. Data from clusters without FA is from our previous studies.[45,46].

Table 2 shows the free energy gain upon adding another acid to the following clusters: $(SA)_1(base)_{1-2}$, $(MSA)_1(base)_{1-2}$ and $(FA)_1(base)_{1-2}$. The results show that it is generally preferred to add the same type of acid to a given cluster rather than FA. For instance, for SA clusters it is more favorable to add another SA molecule compared to adding FA. Positive

https://doi.org/10.1021/acsomega.3c00251
ACS Omega 2023, 8, 9621−9629

Table 3. Calculated Binding Free Energies at the DLPNO−CCSD(T_0)/aug-cc-pVTZ//ωB97X-D/6-31++G(d,p) Level of Theory with the Quasi-harmonic Approximation at 298.15 K, 1 atm (Units Are kcal/mol)

	classification	$(SA)_2(FA)_1$	$(MSA)_2(FA)_1$	$(SA)_1(MSA)_1(FA)_1$
$(A)_2$	w, w	−32.1	−25.2	−30.1
$(MA)_2$	m, m	−42.7	−34.5	−40.5
$(DMA)_2$	s, s	−47.7	−38.6	−45.1
$(TMA)_2$	s, s	−42.7	−26.9	−36.9
$(EDA)_2$	s, s	−45.3	−38.6	−42.9
$(A)_1(MA)_1$	w, m	−37.4	−30.5	−36.2
$(A)_1(DMA)_1$	w, s	−42.7	−34.6	−39.8
$(A)_1(TMA)_1$	w, s	−38.5	−28.8	−41.7
$(A)_1(EDA)_1$	w, s	−40.5	−32.3	−36.7
$(MA)_1(DMA)_1$	m, s	−47.3	−39.0	−42.5
$(MA)_1(TMA)_1$	m, s	−44.2	−34.3	−39.3
$(MA)_1(EDA)_1$	m, s	−45.7	−37.7	−42.1
$(DMA)_1(TMA)_1$	s, s	−46.7	−35.3	−42.7
$(DMA)_1(EDA)_1$	s, s	−47.3	−39.3	−44.2
$(TMA)_1(EDA)_1$	s, s	−44.7	−34.1	−46.5

addition free energies are only observed for the addition of FA to $(FA)_1(TMA)_1$ and $(FA)_1(EDA)_1$. Noteworthy is the value of the addition free energies of FA to the SA and MSA containing dimers with A, MA, or DMA as a base. These indicate that FA is able to greatly stabilize these smaller clusters. The addition of FA is still not stabilizing to the same extent as adding SA or MSA, however taking into account the high vapor concentration of FA, it may support the idea of FA being able to enhance these clusters.

Similarly to our previous study on NA we have expanded our systems to include $(acid)_3(base)_2$ with at least one of the acids being FA. The binding free energies are shown in Table 3 with the following order for stability: $(MSA)_2(FA)_1(base)_2$ < $(SA)_1(MSA)_1(FA)_1(base)_2$ < $(SA)_2(FA)_1(base)_2$. The binding free energy of the clusters are all very low and with the same trend as for the smaller clusters in which clusters containing EDA and DMA form the most stable clusters. Steric effects are still present as TMA-containing clusters are shown to be higher in binding free energy compared to those clusters without TMA but comparable basicity.

The free energy of acid addition for larger systems is presented in Table 4. Similarly, for the case of NA, the addition of FA to these larger clusters are still thermodynamically preferable and for some of the clusters exhibit a stabilizing effect comparable to those presented in Table 2. The same stabilizing effect is not seen to the same extend with no general trend observed for the addition free energy for these larger clusters. Some systems exhibit a large stabilizing effect such as $(SA)_1(MSA)_1(FA)_1(A)_1(TMA)_1$ and $(SA)_1(MSA)_1(FA)_1(TMA)_1(EDA)_1$ with addition free energies of −12.1 and −10.9 kcal mol^{-1}, respectively. However, similar systems such as $(SA)_1(MSA)_1(FA)_1(DMA)_1(TMA)_1$ only measure an addition free energy of −4.2 kcal mol^{-1}.

3.3. Cluster Formation Potential. While the thermochemistry describes the stability of a given cluster, the gas-phase concentration is a cofactor in determining the formation potential of said cluster. FA is one of the most abundant organic acids in the atmosphere and is therefore expected to enhance the formation potential of clusters. Therefore we have simulated the cluster formation potential ($J_{potential}$) of the studied systems using ACDC. The concentration of SA and MSA were kept at 1×10^6 molecules cm^{-3}, while that of FA is set to 2.46×10^{11} (10 ppb). The base concentrations are set to atmospheric relevant concentrations: A (10 ppt−10 ppb), MA (1−100 ppt), DMA (1−10 ppt), TMA (1−10 ppt), and EDA (1−10 ppt). The results are presented in Table 5.

Table 4. Addition Free Energies at the DLPNO−CCSD(T_0)/aug-cc-pVTZ//ωB97X-D/6-31++G(d,p) Level of Theory with the Quasi-harmonic Approximation at 298.15 K, 1 atm (Units Are kcal/mol)[a]

initial cluster:	$(SA)_2$[45]	$(MSA)_2$[46]	$(SA)_1(MSA)_1$[34]
added acid:	(FA)	(FA)	(FA)
$(A)_2$	−5.1	−4.7	−6.5
$(MA)_2$	−6.1	−3.0	−6.7
$(DMA)_2$	−3.7	−2.0	−3.3
$(TMA)_2$	−1.2	−1.3	−5.0
$(EDA)_2$	−3.5	−4.2	−7.1
$(A)_1(MA)_1$	−5.0	−4.4	−3.8
$(A)_1(DMA)_1$	−8.0	−5.7	−6.8
$(A)_1(TMA)_1$	−6.2	−5.7	−12.1
$(A)_1(EDA)_1$	−6.8	−5.0	−4.5
$(MA)_1(DMA)_1$	−6.7	−5.2	−4.1
$(MA)_1(TMA)_1$	−6.1	−6.2	−3.7
$(MA)_1(EDA)_1$	−6.6	−5.5	−5.4
$(DMA)_1(TMA)_1$	−4.4	−4.6	−4.2
$(DMA)_1(EDA)_1$	−3.9	−3.9	−3.5
$(TMA)_1(EDA)_1$	−2.0	−4.5	−10.9

[a]Calculated as the initial cluster binding free energy subtracted from the binding free energy of the cluster with the added acid. Data from clusters without FA are from our previous studies.[34,45,46].

Likewise in our previous studies, the cluster formation potential for the MSA-containing clusters is very low for both the lower and upper limits for base concentration. As outlined in the thermochemistry section these clusters suffer from low stability due to a lack of sufficient accommodation of steric effects and weaker hydrogen bonding compared to their cluster counterpart with SA. This results in the studied clusters containing MSA being less likely to form clusters compared to SA. Additionally, the cluster formation potential for SA−FA−A and FA−SA−MA clusters is also found to be relatively low at both lower and upper concentration limits. This is despite the fact that the concentrations of A and MA are orders of magnitude higher than the other bases. Among the studied clusters, TMA has the highest cluster formation potential, with

https://doi.org/10.1021/acsomega.3c00251
ACS Omega 2023, 8, 9621−9629

Table 5. Simulated Cluster Formation Potential ($J_{potential}$, cm^{-3} s^{-1})

cluster system	lower limit	upper limit
ammonia (A)	**10 ppt**	**10 ppb**
FA−SA−A	4.10×10^{-5}	9.14×10^{-1}
FA−MSA−A	4.80×10^{-10}	4.78×10^{-4}
methylamine (MA)	**1 ppt**	**100 ppt**
FA−SA−MA	7.76×10^{-4}	8.06×10^{-2}
FA−MSA−MA	1.30×10^{-6}	4.13×10^{-3}
dimethylamine (DMA)	**1 ppt**	**10 ppt**
FA−SA−DMA	1.57	15.8
FA−MSA−DMA	6.49×10^{-4}	1.05×10^{-2}
triethylamine (TMA)	**1 ppt**	**10 ppt**
FA−SA−TMA	9.67	81.8
FA−MSA−TMA	8.85×10^{-8}	8.85×10^{-6}
ethylenediamine (EDA)	**1 ppt**	**10 ppt**
FA−SA−EDA	2.61×10^{-1}	2.67
FA−MSA−EDA	8.21×10^{-4}	8.97×10^{-3}

formation rates of 9.67 and 81.8 cm^{-3} s^{-1} at the lower and upper limits, respectively. DMA and EDA have lower cluster formation potentials but still exhibited non-negligible values. The formation rates of DMA, TMA, and EDA all increased by a factor of approximately 10 when going from the lower to the upper limit.

Despite the relatively high cluster formation potential, almost all the observed collisions in the simulations involve $(SA)_2(base)_2 + (FA)_1$ and $(MSA)_2(base)_2 + (FA)_1$ as seen in Table S1 in the Supporting Information. This is due to the high concentration of FA in the simulation. When a stable $(SA)_2(base)_2$ or $(MSA)_2(base)_2$ cluster is formed, it is likely to collide with the abundant FA. However, none of the clusters that collide with FA initially contain FA, indicating that FA evaporates quickly from the cluster in the simulation due to weak interactions within the cluster. The inability to stabilize these smaller clusters in the simulation suggests that clusters of the type $(acid)_2(FA)_1(base)_2$, that is the main types of clusters coming out of the simulation, are unlikely to exist in that composition as FA will likely evaporate as the cluster is formed. This is supported by the addition free energies of FA to the $(acid)_2(base)_2$ clusters (shown in Table 4), which indicates that FA contributes only a small lowering in the cluster's binding free energy.

3.4. Enhancement in $J_{potential}$. The cluster formation potentials ($J_{potential}$) of the FA−SA/MSA−base clusters can be compared to those of the SA/MSA−base clusters to assess the effect of including FA in the cluster formation. The enhancement factor is calculated as

$$R_{FA} = \frac{J_{potential}(\text{FA−SA/MSA−base})}{J_{potential}(\text{SA/MSA−base})} \quad (2)$$

The enhancement factor for the studied clusters is shown in Table 6. Some systems have very high enhancement factors due to dividing two formation potentials that are essentially zero. These systems have been marked as "not applicable" (n/a) in the table and the numbers can be found in the Supporting Information. As a consequence, the enhancement rate is shown to be orders of magnitude for the systems FA−SA/MSA−A at both low and high concentration limit and for FA−SA−MA at the lower limit. FA−MSA−TMA and FA−MSA−EDA also show unrealistic enhancements at both lower and upper concentration limit, caused by the instability of MSA−TMA/EDA clusters. Their cluster formation potentials are still essentially zero and the formation of these clusters is negligible.

Table 6. Enhancement (R_{FA}) in the Simulated Cluster Formation Potential by Having FA Present[a]

cluster system	lower limit	upper limit
ammonia (A)	**10 ppt**	**10 ppb**
FA−SA−A	n/a	n/a
FA−MSA−A	n/a	n/a
methylamine (MA)	**1 ppt**	**100 ppt**
FA−SA−MA	n/a	3.82
FA−MSA−MA	n/a	1.47
dimethylamine (DMA)	**1 ppt**	**10 ppt**
FA−SA−DMA	2.72	2.08
FA−MSA−DMA	10.0	4.66
triethylamine (TMA)	**1 ppt**	**10 ppt**
FA−SA−TMA	17.9	3.74
FA−MSA−TMA	n/a	n/a
ethylenediamine (EDA)	**1 ppt**	**10 ppt**
FA−SA−EDA	6.05	2.49
FA−MSA−EDA	n/a	n/a

[a]Non-FA data were taken from Clusteromic III.[34] The simulations are performed at 278.15 K.

Instead, the focus is directed toward those FA−SA−base systems which showed high non-negligible cluster formation potentials in Table 5, namely, FA−SA−DMA, FA−SA−TMA, and FA−SA−EDA. As mentioned in the previous section, the outgrowing clusters mainly consisted of $(SA)_2(base)_2 + (FA)_1$, indicating FA does not significantly stabilize the initial cluster formation. To test this, the main collision pathway $(SA)_2(base)_2 + (FA)_1$ out of the simulation is disabled to see how the cluster formation potential changed. For the SA−FA−DMA system, the cluster formation potential changed to 0.583 and 8.09 cm^{-3} s^{-1} for the lower and upper limits, respectively. This corresponds to an enhancement factor of 1.16 and 1.21 for the lower and upper limits, respectively. Reducing the enhancement factor that FA initially showed by around a factor of 2. Considering 298.15 K, the enhancement factor in the lower and upper limits drop to 1.01 and 1.01, respectively. The opposite is observed when lowering the temperature to 258.15 K, where the enhancement factor in the lower and upper limits highly increases to 4.28 and 70, respectively. For the SA−FA−EDA system, the cluster formation potential is reduced to 0.046 and 1.15 cm^{-3} s^{-1} for the lower and upper limits, respectively. Corresponding to an enhancement factor of 1.08 for both the lower and upper limits. Lastly, the SA−FA−TMA system which initially showed the greatest cluster formation potential had a reduction to 0.503 and 21.9 cm^{-3} s^{-1} for lower and upper limits, respectively. This is an enhancement factor equal to 1, indicating that FA has no enhancing effect on the cluster formation between SA and TMA. FA only showed a very slight enhancement of the cluster formation potential of the FA−SA−DMA and FA−SA−EDA systems. Assuming then, that FA in the larger clusters is not stable enough to withstand evaporation, the large enhancement factors in Table 6 are mostly a result of the increased acid vapor in the simulations, as opposed to FA being able to form stable interactions within the studied systems. Only SA−FA−DMA of the three systems showed a considerable enhancement in cluster formation potential as well as 5% of the collisions being attributed to

https://doi.org/10.1021/acsomega.3c00251
ACS Omega 2023, 8, 9621−9629

$(SA)_1(FA)_1(DMA)_2$ + $(FA)_1$ when the major $(SA)_2(DMA)_2$ + $(FA)_1$ pathway is turned off.

4. CONCLUSIONS

Computational methods have been used to study the thermodynamics and cluster formation properties of various acid−base clusters using the DLPNO-CCSD(T_0)/aug-cc-pVTZ//ωB97X-D/6-31++G(d,p) method and the quasi-harmonic approximation at 298.15 K, 1 atm, and a vibrational frequency cutoff of 100 cm^{-1}. The acid components considered included formic acid (FA), sulfuric acid (SA), and methanesulfonic acid (MSA), while the base components included ammonia (A), methylamine (MA), dimethylamine (DMA), trimethylamine (TMA), and ethylenediamine (EDA). The thermochemical results were shown to be in line with previous studies, showing that the most stable clusters contained SA and a combination of the strong bases DMA, TMA, and EDA. Sterical effects were shown to be present in the smaller clusters, however to a lesser extent when compared to the larger clusters. Likewise, an aversion for TMA in the clusters was observed, especially for the MSA clusters. The addition free energy of FA was shown to be less than that of adding SA or MSA to their respective clusters. Furthermore, as the clusters became larger the addition free energy of FA decreased, as well. Cluster dynamics simulations initially showed that the cluster formation potential of FA−SA−base and FA−MSA−base clusters was significantly enhanced compared to the non-FA counterparts. However, this effect was largely due to collisions between stable SA/MSA−base clusters with FA. As these SA/MSA−FA−base clusters would most likely subsequently lose formic acid through evaporation, the cluster configurations coming out of the simulation are too unstable to exist in the atmosphere. Of the studied systems with a significant cluster formation potential, only the FA−SA−DMA and FA−SA−EDA systems present a significant enhancement of cluster formation by FA, with the FA−SA−DMA system showing the largest enhancement at around 21%. For the studied systems FA is therefore only expected to enhance the SA−DMA cluster formation at the studied conditions. While this study has only examined the role of FA in systems consisting of SA, MSA, and bases, it is likely that the cumulative effects of organic acids in the atmosphere will lead to the enhancement of cluster formation greater than what has been demonstrated in this study.

■ ASSOCIATED CONTENT

Supporting Information

The Supporting Information is available free of charge at https://pubs.acs.org/doi/10.1021/acsomega.3c00251.

Clusters leaving the simulation box, contributing to $J_{potential}$; cluster formation potential at 298.15 K; enhancement factors at 278.15 and 298.15 K (PDF)

■ AUTHOR INFORMATION

Corresponding Author

Jonas Elm − *Department of Chemistry, iClimate, Aarhus University, 8000 Aarhus C, Denmark;* orcid.org/0000-0003-3736-4329; Phone: +45 28938085; Email: jelm@chem.au.dk

Authors

Daniel Ayoubi − *Department of Chemistry, Aarhus University, 8000 Aarhus C, Denmark*

Yosef Knattrup − *Department of Chemistry, Aarhus University, 8000 Aarhus C, Denmark;* orcid.org/0000-0003-3549-7494

Complete contact information is available at: https://pubs.acs.org/10.1021/acsomega.3c00251

Notes

The authors declare no competing financial interest.

■ ACKNOWLEDGMENTS

The authors thank the Independent Research Fund Denmark Grant No. 9064-00001B for financial support. The numerical results presented in this work were obtained at the Centre for Scientific Computing, Aarhus http://phys.au.dk/forskning/cscaa/.

■ REFERENCES

(1) Haywood, J.; Boucher, O. Estimates of the Direct and Indirect Radiative Forcing due to Tropospheric Aerosols: A Review. *Rev. Geophys.* **2000**, *38*, 513−543.

(2) Lohmann, U.; Feichter, J. Global indirect aerosol effects: A review. *Atmos. Phys. Chem.* **2005**, *5*, 715−737.

(3) Merikanto, J.; Spracklen, D. V.; Mann, G. W.; Pickering, S. J.; Carslaw, K. S. Impact of nucleation on global CCN. *Atmos. Chem. Phys.* **2009**, *9*, 8601−8616.

(4) *IPCC, 2013: Climate Change 2013: The Physical Science Basis. Contribution of Working Group I to the Fifth Assessment Report of the Intergovernmental Panel on Climate Change*; Stocker, T. F., Qin, D., Plattner, G.-K., Tignor, M., Allen, S. K., Boschung, J., Nauels, A., Xia, Y., Bex, V., Midgley, P. M., Eds.; Cambridge University Press: Cambridge, UK, 2013; 1535 pp.

(5) Sipilä, M.; Berndt, T.; Petäjä, T.; Brus, D.; Vanhanen, J.; Stratmann, F.; Patokoski, J.; Mauldin, R. L.; Hyvärinen, A.-P.; Lihavainen, H.; Kulmala, M. The Role of Sulfuric Acid in Atmospheric Nucleation. *Science* **2010**, *327*, 1243−1246.

(6) Kirkby, J.; Curtius, J.; Almeida, J.; Dunne, E.; Duplissy, J.; Ehrhart, S.; Franchin, A.; Gagné, S.; Ickes, L.; Kürten, A.; Kupc, A.; Metzger, A.; Riccobono, F.; Rondo, L.; Schobesberger, S.; Tsagkogeorgas, G.; Wimmer, D.; Amorim, A.; Bianchi, F.; Breitenlechner, M.; David, A.; Dommen, J.; Downard, A.; Ehn, M.; Flagan, R. C.; Haider, S.; Hansel, A.; Hauser, D.; Jud, W.; Junninen, H.; Kreissl, F.; Kvashin, A.; Laaksonen, A.; Lehtipalo, K.; Lima, J.; Lovejoy, E. R.; Makhmutov, V.; Mathot, S.; Mikkilä, J.; Minginette, P.; Mogo, S.; Nieminen, T.; Onnela, A.; Pereira, P.; Petäjä, T.; Schnitzhofer, R.; Seinfeld, J. H.; Sipilä, M.; Stozhkov, Y.; Stratmann, F.; Tomé, A.; Vanhanen, J.; Viisanen, Y.; Vrtala, A.; Wagner, P. E.; Walther, H.; Weingartner, E.; Wex, H.; Winkler, P. M.; Carslaw, K. S.; Worsnop, D. R.; Baltensperger, U.; Kulmala, M. Role of Sulphuric Acid, Ammonia and Galactic Cosmic Rays in Atmospheric Aerosol Nucleation. *Nature* **2011**, *476*, 429−433.

(7) Almeida, J.; Schobesberger, S.; Kürten, A.; Ortega, I. K.; Kupiainen-Määttä, O.; Praplan, A. P.; Adamov, A.; Amorim, A.; Bianchi, F.; Breitenlechner, M.; et al. Molecular Understanding of Sulphuric Acid-Amine Particle Nucleation in the Atmosphere. *Nature* **2013**, *502*, 359−363.

(8) Kurtén, T.; Sundberg, M. R.; Vehkamäki, H.; Noppel, M.; Blomqvist, J.; Kulmala, M. Ab Initio and Density Functional Theory Reinvestigation of Gas-Phase Sulfuric Acid Monohydrate and Ammonium Hydrogen Sulfate. *J. Phys. Chem. A* **2006**, *110*, 7178−7188.

(9) Kurtén, T.; Torpo, L.; Sundberg, M. R.; Kerminen, V.; Vehkamäki, H.; Kulmala, M. Estimating the NH_3:H_2SO_4 Ratio of Nucleating Clusters in Atmospheric Conditions using Quantum Chemical Methods. *Atmos. Chem. Phys.* **2007**, *7*, 2765−2773.

(10) Kurtén, T.; Torpo, L.; Ding, C.; Vehkamäki, H.; Sundberg, M. R.; Laasonen, K.; Kulmala, M. A Density Functional Study on Water-Sulfuric Acid-ammonia Clusters and Implications for Atmospheric Cluster Formation. *J. Geophys. Res.* **2007**, *112*, D04210.
(11) Torpo, L.; Kurtén, T.; Vehkamäki, H.; Laasonen, K.; Sundberg, M. R.; Kulmala, M. Significance of Ammonia in Growth of Atmospheric Nanoclusters. *J. Phys. Chem. A* **2007**, *111*, 10671−10674.
(12) Kurtén, T.; Loukonen, V.; Vehkamäki, H.; Kulmala, M. Amines are Likely to Enhance Neutral and Ion-induced Sulfuric Acid-water Nucleation in the Atmosphere More Effectively than Ammonia. *Atmos. Chem. Phys.* **2008**, *8*, 4095−4103.
(13) Nadykto, A. B.; Yu, F.; Jakovleva, M. V.; Herb, J.; Xu, Y. Amines in the Earth's Atmosphere: A Density Functional Theory Study of the Thermochemistry of Pre-Nucleation Clusters. *Entropy* **2011**, *13*, 554−569.
(14) Herb, J.; Nadykto, A. B.; Yu, F. Large Ternary Hydrogen-bonded Pre-nucleation Clusters in the Earth's Atmosphere. *Chem. Phys. Lett.* **2011**, *518*, 7−14.
(15) Ortega, I. K.; Kupiainen, O.; Kurtén, T.; Olenius, T.; Wilkman, O.; McGrath, M. J.; Loukonen, V.; Vehkamäki, H. From Quantum Chemical Formation Free Energies to Evaporation Rates. *Atmos. Chem. Phys.* **2012**, *12*, 225−235.
(16) Nadykto, A. B.; Herb, J.; Yu, F.; Xu, Y. Enhancement in the Production of Nucleating Clusters due to Dimethylamine and Large Uncertainties in the Thermochemistry of Amine-Enhanced Nucleation. *Chem. Phys. Lett.* **2014**, *609*, 42−49.
(17) DePalma, J. W.; Doren, D. J.; Johnston, M. V. Formation and Growth of Molecular Clusters Containing Sulfuric Acid, Water, Ammonia, and Dimethylamine. *J. Phys. Chem. A* **2014**, *118*, 5464−5473.
(18) Nadykto, A. B.; Herb, J.; Yu, F.; Xu, Y.; Nazarenko, E. S. Estimating the Lower Limit of the Impact of Amines on Nucleation in the Earth's Atmosphere. *Entropy* **2015**, *17*, 2764−2780.
(19) Elm, J. Elucidating the Limiting Steps in Sulfuric Acid - Base New Particle Formation. *J. Phys. Chem. A* **2017**, *121*, 8288−8295.
(20) Elm, J.; Passananti, M.; Kurtén, T.; Vehkamäki, H. Diamines Can Initiate New Particle Formation in the Atmosphere. *J. Phys. Chem. A* **2017**, *121*, 6155−6164.
(21) Myllys, N.; Kubečka, J.; Besel, V.; Alfaouri, D.; Olenius, T.; Smith, J. N.; Passananti, M. Role of Base Strength, Cluster Structure and Charge in Sulfuric Acid-Driven Particle Formation. *Atmos. Chem. Phys.* **2019**, *19*, 9753−9768.
(22) Chen, D.; Li, D.; Wang, C.; Liu, F.; Wang, W. Formation Mechanism of Methanesulfonic Acid and Ammonia Clusters: A Kinetics Simulation Study. *Atmos. Environ.* **2020**, *222*, 117161.
(23) Chen, D.; Li, D.; Wang, C.; Luo, Y.; Liu, F.; Wang, W. Atmospheric Implications of Hydration on the Formation of Methanesulfonic Acid and Methylamine Clusters: A Theoretical Study. *Chemosphere* **2020**, *244*, 125538.
(24) Shen, J.; Xie, H.; Elm, J.; Ma, F.; Chen, J.; Vehkamäki, H. Methanesulfonic Acid-driven New Particle Formation Enhanced by Monoethanolamine: A Computational Study. *Environ. Sci. Technol.* **2019**, *53*, 14387−14397.
(25) Dawson, M. L.; Varner, M. E.; Perraud, V.; Ezell, M. J.; Gerber, R. B.; Finlayson-Pitts, B. J. Simplified Mechanism for New Particle Formation from Methanesulfonic Acid, Amines, and Water Via Experiments and Ab Initio Calculations. *Proc. Natl. Acad. Sci. U.S.A.* **2012**, *109*, 18719−18724.
(26) Chen, H. H.; Ezell, M. J.; Arquero, K. D.; Varner, M. E.; Dawson, M. L.; Gerber, R. B.; Finlayson-Pitts, B. J. New Particle Formation and Growth from Methanesulfonic Acid, Trimethylamine and Water. *Phys. Chem. Chem. Phys.* **2015**, *17*, 13699−13709.
(27) Chen, H. H.; Finlayson-Pitts, B. J. New Particle Formation from Methanesulfonic Acid and Amines/ammonia as a Function of Temperature. *Environ. Sci. Technol.* **2017**, *51*, 243−252.
(28) Arquero, K. D.; Gerber, R. B.; Finlayson-Pitts, B. J. The Role of Oxalic Acid in New Particle Formation from Methanesulfonic Acid, Methylamine, and Water. *Environ. Sci. Technol.* **2017**, *51*, 2124−2130.
(29) Arquero, K. D.; Xu, J.; Gerber, R. B.; Finlayson-Pitts, B. J. Particle Formation and Growth from Oxalic Acid, Methanesulfonic Acid, Trimethylamine and Water: A Combined Experimental and Theoretical Study. *Phys. Chem. Chem. Phys.* **2017**, *19*, 28286−28301.
(30) Shen, J.; Elm, J.; Xie, H.; Chen, J.; Niu, J.; Vehkamäki, H. Structural Effects of Amines in Enhancing Methanesulfonic Acid-Driven New Particle Formation. *Environ. Sci. Technol.* **2020**, *54*, 13498−13508.
(31) Perraud, V.; Xu, J.; Gerber, R. B.; Finlayson-Pitts, B. J. Integrated Experimental and Theoretical Approach to Probe the Synergistic Effect of Ammonia in Methanesulfonic Acid Reactions with Small Alkylamines. *Environ. Sci.: Processes Impacts* **2020**, *22*, 305−328.
(32) Chen, D.; Wang, W.; Li, D.; Wang, W. Atmospheric Implication of Synergy in Methanesulfonic Acid-base Trimers: A Theoretical Investigation. *RSC Adv.* **2020**, *10*, 5173−5182.
(33) Bork, N.; Elm, J.; Olenius, T.; Vehkamäki, H. Methane Sulfonic Acid-enhanced Formation of Molecular Clusters of Sulfuric Acid and Dimethyl Amine. *Atmos. Chem. Phys.* **2014**, *14*, 12023−12030.
(34) Elm, J. Clusteromics III: Acid Synergy in Sulfuric Acid-Methanesulfonic Acid-Base Cluster Formation. *ACS Omega* **2022**, *7*, 15206−15214.
(35) Knattrup, Y.; Elm, J. Clusteromics IV: The Role of Nitric Acid in Atmospheric Cluster Formation. *ACS Omega* **2022**, *7*, 31551−31560.
(36) Zhang, R.; Suh, I.; Zhao, J.; Zhang, D.; Fortner, E. C.; Tie, X.; Molina, L. T.; Molina, M. J. Atmospheric New Particle Formation Enhanced by Organic Acids. *Science* **2004**, *304*, 1487−1490.
(37) Nadykto, A. B.; Yu, F. Strong Hydrogen Bonding Between Atmospheric Nucleation Precursors and Common Organics. *Chem. Phys. Lett.* **2007**, *435*, 14−18.
(38) Khwaja, H. A. Atmospheric Concentrations of Carboxylic Acids and Related Compounds at a Semiurban Site. *Atmos. Environ.* **1995**, *29*, 127−139.
(39) Yan, J.; Jung, J.; Zhang, M.; Xu, S.; Lin, Q.; Zhao, S.; Chen, L. Significant Underestimation of Gaseous Methanesulfonic Acid (MSA) over Southern Ocean. *Environ. Sci. Technol.* **2019**, *53*, 13064−13070.
(40) Baccarini, A.; Karlsson, L.; Dommen, J.; Duplessis, P.; Vüllers, J.; Brooks, I. M.; Saiz-Lopez, A.; Salter, M.; Tjernström, M.; Baltensperger, U.; Zieger, P.; Schmale, J. Frequent New Particle Dormation Over the High Arctic Pack Ice by Enhanced Iodine Emissions. *Nat. Commun.* **2020**, *11*, 4924.
(41) Beck, L. J.; Sarnela, N.; Junninen, H.; Hoppe, C. J. M.; Garmash, O.; Bianchi, F.; Riva, M.; Rose, C.; Peräkylä, O.; Wimmer, D.; Kausiala, O.; Jokinen, T.; Ahonen, L.; Mikkilä, J.; Hakala, J.; He, X.-C.; Kontkanen, J.; Wolf, K. K. E.; Cappelletti, D.; Mazzola, M.; Traversi, R.; Petroselli, C.; Viola, A. P.; Vitale, V.; Lange, R.; Massling, A.; Nøjgaard, J. K.; Krejci, R.; Karlsson, L.; Zieger, P.; Jang, S.; Lee, K.; Vakkari, V.; Lampilahti, J.; Thakur, R. C.; Leino, K.; Kangasluoma, J.; Duplissy, E.-M.; Siivola, E.; Marbouti, M.; Tham, Y. J.; Saiz-Lopez, A.; Petäjä, T.; Ehn, M.; Worsnop, D. R.; Skov, H.; Kulmala, M.; Kerminen, V.-M.; Sipilä, M. Differing Mechanisms of New Particle Formation at Two Arctic Sites. *Geophys. Res. Lett.* **2021**, *48*, e2020GL091334.
(42) Harold, S. E.; Bready, C. J.; Juechter, L. A.; Kurfman, L. A.; Vanovac, S.; Fowler, V. R.; Mazaleski, G. E.; Odbadrakh, T. T.; Shields, G. C. Hydrogen-Bond Topology Is More Important Than Acid/Base Strength in Atmospheric Prenucleation Clusters. *J. Phys. Chem. A.* **2022**, *126*, 1718−1728.
(43) Zhang, R.; Jiang, S.; Liu, Y.-R.; Wen, H.; Feng, Y.-J.; Huang, T.; Huang, W. An Investigation About the Structures, Thermodynamics and Kinetics of the Formic Acid Involved Molecular Clusters. *Chem. Phys.* **2018**, *507*, 44−50.
(44) Zhang, R.; Shen, J.; Xie, H.-B.; Chen, J.; Elm, J. The Role of Organic Acids in New Particle Formation From Methanesulfonic Acid and Methylamine. *Atmos. Chem. Phys.* **2022**, *22*, 2639−2650.
(45) Elm, J. Clusteromics I: Principles, Protocols and Applications to Sulfuric Acid - Base Cluster Formation. *ACS Omega* **2021**, *6*, 7804−7814.

https://doi.org/10.1021/acsomega.3c00251
ACS Omega 2023, 8, 9621−9629

(46) Elm, J. Clusteromics II: Methanesulfonic Acid-Base Cluster Formation. *ACS Omega* **2021**, *6*, 17035−17044.
(47) Stewart, J. J. P. Optimization of Parameters for Semiempirical Methods VI: More Modifications to the NDDO Approximations and Re-optimization of Parameters. *J. Mol. Model.* **2013**, *19*, 1−32.
(48) Frisch, M. J.; Trucks, G. W.; Schlegel, H. B.; Scuseria, G. E.; Robb, M. A.; Cheeseman, J. R.; Scalmani, G.; Barone, V.; Petersson, G. A.; Nakatsuji, H.; et al. *Gaussian 16*, revision A.03; Gaussian, Inc.: Wallingford, CT, 2016.
(49) Frisch, M. J., Trucks, G. W., Schlegel, H. B., Scuseria, G. E., Robb, M. A., Cheeseman, J. R., Scalmani, G., Barone, V., Mennucci, B., Petersson, G. A.; et al. *Gaussian 09*, revision B.01; Gaussian, Inc.: Wallingford, CT, 2010.
(50) Elm, J. An Atmospheric Cluster Database Consisting of Sulfuric Acid, Bases, Organics, and Water. *ACS Omega* **2019**, *4*, 10965−10974.
(51) Neese, F. *WIREs Comput. Mol. Sci.* **2012**, *2*, 73−78.
(52) Neese, F. Software update: the ORCA program system, version 4.0. *WIREs Comput. Mol. Sci.* **2018**, *8* (1), e1327.
(53) Riplinger, C.; Neese, F. An Efficient and Near Linear Scaling Pair Natural Orbital Based Local Coupled Cluster Method. *J. Chem. Phys.* **2013**, *138*, 034106.
(54) Riplinger, C.; Sandhoefer, B.; Hansen, A.; Neese, F. Natural Triple Excitations in Local Coupled Cluster Calculations with Pair Natural Orbitals. *J. Chem. Phys.* **2013**, *139*, 134101.
(55) Liakos, D. G.; Sparta, M.; Kesharwani, M. K.; Martin, J. M. L.; Neese, F. Exploring the Accuracy Limits of Local Pair Natural Orbital Coupled-Cluster Theory. *J. Chem. Theory. Comput.* **2015**, *11*, 1525−1539.
(56) Chai, J.-D.; Head-Gordon, M. Long-Range Corrected Hybrid Density Functionals with Damped Atom-Atom Dispersion Corrections. *Phys. Chem. Chem. Phys.* **2008**, *10*, 6615−6620.
(57) Elm, J.; Mikkelsen, K. V. Computational Approaches for Efficiently Modelling of Small Atmospheric Clusters. *Chem. Phys. Lett.* **2014**, *615*, 26−29.
(58) Myllys, N.; Elm, J.; Kurtén, T. Density Functional Theory Basis Set Convergence of Sulfuric Acid-Containing Molecular Clusters. *Comp. Theor. Chem.* **2016**, *1098*, 1−12.
(59) Elm, J.; Bilde, M.; Mikkelsen, K. V. Assessment of Density Functional Theory in Predicting Structures and Free Energies of Reaction of Atmospheric Prenucleation Clusters. *J. Chem. Theory Comput.* **2012**, *8*, 2071−2077.
(60) Elm, J.; Kristensen, K. Basis Set Convergence of the Binding Energies of Strongly Hydrogen-Bonded Atmospheric Clusters. *Phys. Chem. Chem. Phys.* **2017**, *19*, 1122−1133.
(61) Schmitz, G.; Elm, J. Assessment of the DLPNO Binding Energies of Strongly Non-covalent Bonded Atmospheric Molecular Clusters. *ACS Omega* **2020**, *5*, 7601−7612.
(62) Grimme, S. Supramolecular Binding Thermodynamics by Dispersion-corrected Density Functional Theory. *Chem.—Eur. J.* **2012**, *18*, 9955−9964.
(63) Funes-Ardois, I.; Paton, R. *GoodVibes v1.0.1* 2016; DOI: 10.5281/zenodo.60811.
(64) Elm, J.; Kubečka, J.; Besel, V.; Jääskeläinen, M. J.; Halonen, R.; Kurtén, T.; Vehkamäki, H. Modeling the Formation and Growth of Atmospheric Molecular Clusters: A Review. *J. Aerosol. Sci.* **2020**, *149*, 105621.
(65) Zhang, J.; Dolg, M. ABCluster: The Artificial Bee Colony Algorithm for Cluster Global Optimization. *Phys. Chem. Chem. Phys.* **2015**, *17*, 24173−24181.
(66) Zhang, J.; Dolg, M. Global Optimization of Clusters of Rigid Molecules Using the Artificial Bee Colony Algorithm. *Phys. Chem. Chem. Phys.* **2016**, *18*, 3003−3010.
(67) Kubečka, J.; Besel, V.; Kurtén, T.; Myllys, N.; Vehkamäki, H. Configurational Sampling of Noncovalent (Atmospheric) Molecular Clusters: Sulfuric Acid and Guanidine. *J. Phys. Chem. A* **2019**, *123*, 6022−6033.
(68) Temelso, B.; Mabey, J. M.; Kubota, T.; Appiah-Padi, N.; Shields, G. C. ArbAlign: A Tool for Optimal Alignment of Arbitrarily Ordered Isomers Using the Kuhn−Munkres Algorithm. *J. Chem. Inf. Model* **2017**, *57*, 1045−1054.
(69) Kildgaard, J. V.; Mikkelsen, K. V.; Bilde, M.; Elm, J. Hydration of Atmospheric Molecular Clusters: A New Method for Systematic Configurational Sampling. *J. Phys. Chem. A* **2018**, *122*, 5026−5036.
(70) Kildgaard, J. V.; Mikkelsen, K. V.; Bilde, M.; Elm, J. Hydration of Atmospheric Molecular Clusters II: Organic Acid-Water Clusters. *J. Phys. Chem. A* **2018**, *122*, 8549−8556.
(71) McGrath, M. J.; Olenius, T.; Ortega, I. K.; Loukonen, V.; Paasonen, P.; Kurtén, T.; Kulmala, M.; Vehkamäki, H. Atmospheric Cluster Dynamics Code: A Flexible Method for Solution of the Birth-Death Equations. *Atmos. Chem. Phys.* **2012**, *12*, 2345−2355.
(72) Olenius, T.; Kupiainen-Määttä, O.; Ortega, I. K.; Kurtén, T.; Vehkamäki, H. Free Energy Barrier in the Growth of Sulfuric Acid-Ammonia and Sulfuric Acid-Dimethylamine Clusters. *J. Chem. Phys.* **2013**, *139*, 084312.
(73) Roldin, P.; Ehn, M.; Kurtén, T.; Olenius, T.; Rissanen, M. P.; Sarnela, N.; Elm, J.; Rantala, P.; Hao, L.; Hyttinen, N.; Heikkinen, L.; Worsnop, D. R.; Pichelstorfer, L.; Xavier, C.; Clusius, P.; Ostrom, E.; Petäjä, T.; Kulmala, M.; Vehkamäki, H.; Virtanen, A.; Riipinen, I.; Boy, M. The Role of Highly Oxygenated Organic Molecules in the Boreal Aerosol-cloud-climate System. *Nat. Commun.* **2019**, *10*, 4370.
(74) https://github.com/tolenius/ACDC (accessed 2021-11-01).
(75) Besel, V.; Kubečka, J.; Kurtén, T.; Vehkamäki, H. Impact of Quantum Chemistry Parameter Choices and Cluster Distribution Model Settings on Modeled Atmospheric Particle Formation Rates. *J. Phys. Chem. A* **2020**, *124*, 5931−5943.
(76) Hunter, E. P. L.; Lias, S. G. Evaluated Gas Phase Basicities and Proton Affinities of Molecules: An Update. *J. Phys. Chem. Ref. Data* **1998**, *27*, 413.
(77) Bready, C. J.; Fowler, V. R.; Juechter, L. A.; Kurfman, L. A.; Mazaleski, G. E.; Shields, G. C. The Driving Effects of Common Atmospheric Molecules for Formation of Prenucleation Clusters: The Case of Sulfuric Acid, Formic Acid, Nitric Acid, Ammonia, and Dimethyl Amine. *Environ. sci. Atmos.* **2022**, *2*, 1469−1486.

https://doi.org/10.1021/acsomega.3c00251
ACS Omega 2023, 8, 9621−9629